

Advanced Self Balancing Bridge Accelerometer using Sigma Delta Chip

Anitha Kumari R D
Department of ECE
REVA Institute of Tech and Mgmt,
Katigenahalli, Yelahanka,
Bangalore- 560064

Narendra Reddy P N
Department of ECE
Brindavan college of Engineering,
Dwarakanagar, Yelahanka
Bangalore- 560063

ABSTRACT

This paper presents an advanced self balancing bridge accelerometer with closed loop digital feedback using the sigma delta-chip. Self-balancing bridge reduces the squeeze film damping by introducing the holes in the structure as add on to the proposed structure. The total area of the electrodes is 7.44×10^{-6} as compared to the total area of the holes which is 4.80×10^{-7} with no compromise in the nominal capacitance with holes being incorporated in structure. The main issues that have been achieved are good linearity with respect to the plate deflection and a high dynamic range. Advance self balancing bridge accelerometer has been found to be the optimum solution used to measure plate deflection, symmetrical electrostatic forces on the capacitor plates, its offset and output noise.

Keywords

MEMS, Micro-machine, Bridge Accelerometer.

1. INTRODUCTION

MEMS accelerometers are the simplest and also most applicable micro-electromechanical systems. They became essential in various technologies such as automobile industry, computer and audio-video technology etc. An accelerometer is used to measure electromechanical device that measures acceleration forces such as static, like the constant force of gravity, or they could be dynamic - caused by moving or vibrating the accelerometer. There are many types of accelerometers developed and reported in the literature. The vast majority is based on piezoelectric crystals, but they are too big and too clumsy.

Micro-Accelerometers are micro-machined acceleration sensors with dimensions ranging from 1m to 1mm. They find a wide range of applications, including automotive safety and stability control systems, various navigation and guidance systems, vibration monitoring in industrial environments, movement detection in hand-held mobile terminals and control devices such as game controllers, and different biomedical applications, for example. The readout mechanism of a micro-accelerometer can be, for instance, piezoelectric, piezoresistive or capacitive

[1]. Capacitive accelerometers have advantages such as zero static biasing current, the capability of high sensitivity, and excellent thermal stability, making their use in low-power applications attractive. By using a single capacitive accelerometer with a proper configuration, accelerations along all three axes can be measured simultaneously [2], [3].

The structural element of these devices, together with fixed electrodes, forms four differential capacitor pairs. All three vector components of linear acceleration, x-, y-, and z-directional, can be evaluated by first measuring these capacitances, and then taking their proper linear combinations. Additionally, the configuration provides redundancy so that fault conditions can be detected. The use of micro-sensors in battery-powered equipment requires the sensor interface to exhibit low power dissipation. An inexpensive, yet reliable, highly-sensitive and low-power 3-axis accelerometer with digital output would have a wider range of applications. In order to realize this kind of a sensor, the readout electronics has to be integrated together with the sensor element at chip or module level, forming a micro-electromechanical system (MEMS).

2. ADVANCED SELF BALANCING BRIDGE ACCELEROMETER

Capacitive accelerometers have interesting properties such as high sensitivity, good linearity and low fabrication cost. A vacuum packaged MEMS acceleration sensitive device, i.e., sensor element, has a high quality factor Q due to low air damping. The complexities lie in the measurement of the plate deflection. The main problems addressed here are good linearity with respect to the plate deflection and a high dynamic range. That is the measures of the plate deflection are very low, symmetrical electrostatic forces act on the capacitor plates and the electronic circuit was optimized with respect to its offset and output noise. The self balancing bridge has been found to be the optimum solution.

The accelerometer sensor consists of a central movable plate with fixed electrodes on each side [4]. Together the three electrodes form the capacitors C_1 and C_2 . The plate deflection with respect to distance d_0 between the fixed electrodes may be expressed in terms of the capacitances C_1 and C_2 , by (1)

$$X = \frac{\Delta d}{d_0} = \frac{(C_1 - C_2)}{(C_1 + C_2)} \quad (1)$$

A measurement scheme resulting in a voltage proportional to $(c_1 - c_2) / (c_1 + c_2)$ leads to a linear relationship between the plate deflection and the output voltage. Such a measurement scheme is realized using the advanced self balancing capacitive bridge accelerometers. The fixed electrodes of the capacitor C_1 and C_2 are periodically switched between the reference voltages V_0 and the output voltage V_m .

The resulting charge transfers Q_1 and Q_2 on the capacitors C_1 and C_2 as well as their differences is given by

$$\Delta Q = Q_1 - Q_2 = C_1(V_0 - V_m) - C_2(V_0 + V_m) \quad (2)$$

The measurement circuits sample the ΔQ from the movable center plate and integrate it to a filter capacitor thereby generating the output voltage V_m [5], that is feedback to the excitation network in order to establish the equilibrium condition $\Delta Q=0$.

Typical sensor interface topologies for accelerometers can be divided into two main categories, open-loop and closed-loop. In the open-loop case, no electrostatic force feedback is applied to the sensor element in order to modify its transfer function from acceleration to displacement. While open-loop interface is less complex to implement, it doesn't allow affecting the sensor element properties. Thus, input signal bandwidth (BW), damping and range can be limited by the sensor element. However, an important advantage of the open-loop is that, the output of the interface is linearly proportional to reference voltage used for signal detection, i.e., ratio-metric. When this ratio-metric output is fed to an ADC, which has the same reference as interface, the reference voltage dependence of the sensor output is ideally eliminated.

The schematic of the self balancing capacitor bridge is shown in the figure 1. The circuit consists of an amplifying stage and an integrator formed by (Operational Transconductance Amplifier) OTA1 and OTA2. The clocks control the switches used in the stages. The clock sequence can be roughly divided into SAMPLE and HOLD state. During the HOLD state output voltage V_m remains constant and the voltage potential C_1 , C_2 and C_3 are all discharged through the switches operated by the clock C_2 .

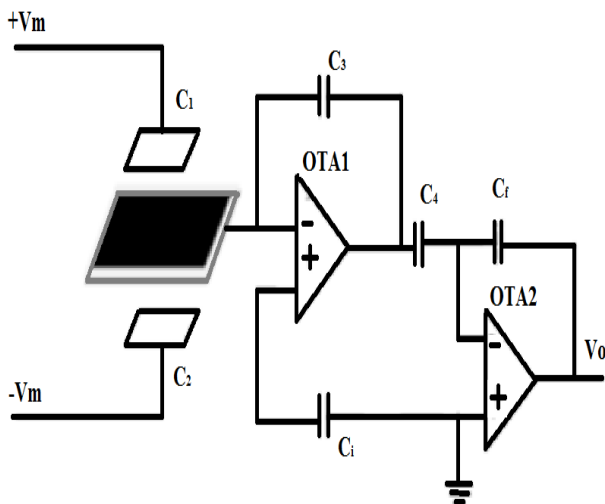


Fig 1: schematic of the self balancing capacitor bridge

In the sample state, the capacitors C_1 and C_2 are charged up to the values $(V_0 - V_m)$ and $(V_0 + V_m)$, respectively. The maximum net flow through the middle electrode as given by the equation is integrated on the capacitor and leads to an error voltage at the output. This error voltage is sampled by capacitor and is integrated on the filter capacitor C_f thereby defining the output voltage V_m of the next measurement cycles.

3. SAMPLE AND HOLD STATE

3.1 Sample State

The capacitors C_1 and C_2 are charged to the supply voltage. The net charge flow through the middle electrode creates an output voltage given by

$$V_0 = V_m * \left(\frac{C_1 - C_2}{C_1 + C_2} \right) * \frac{(C_4 C_0)}{C_3 C_f} = V_m * X * \frac{C_4 C_0}{C_3 C_f} \quad (3)$$

where X = normalized plate deflection

3.2 Hold state

The output voltage is fed back to the excitation network, the net charge on the movable plate is made zero. Here the capacitors C_1 , C_2 and C_3 are all discharged through the switches operated by the clock ck_2 . The amplifier offset $1/f$ noise; charge injection and KT/C noise are stored on capacitor C_4 .

4. CLOSED LOOP ACCELEROMETERS

Open loop accelerometers suffer from cross coupling and are subject to pickoff nonlinearity and hysteresis from their mechanical springs. Pickoffs are needed to measure large displacements so even a low linearity error is crucial. But in closed loop sensors, the displacement is minimal and therefore closed loop accelerometers rely less on pickoff linearity than the open loop.

The open loop accelerometers have limited performance in terms of bandwidth, linearity and dynamic range. Also non linear effects caused by damping and the electrostatic forces required for the signal pickup increase with the deflection of the seismic mass. A feasible method for reducing these nonlinearities is to use closed loop strategy to provide a reset to the seismic mass to keep it at the central position between the electrodes, approximately given by

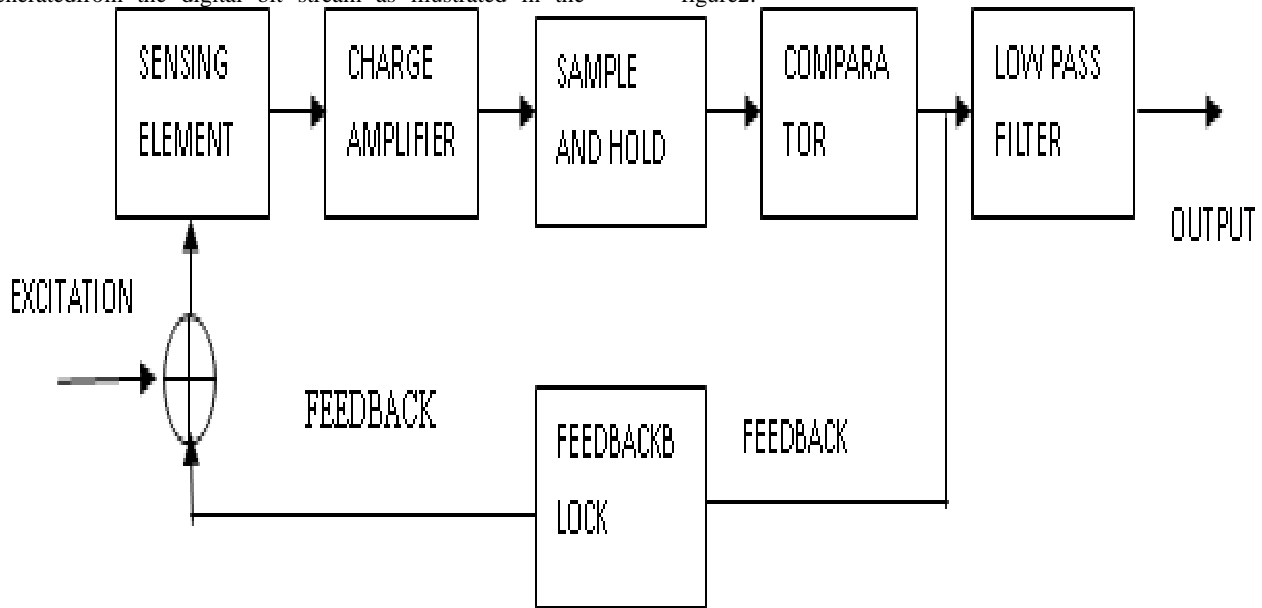
$$\omega_n = \frac{6IE}{mL_{eff}} \quad (4)$$

Now, the force has to be such that it counterbalances the accelerating force and provides an accurate measure of the acceleration (as an error signal). The sensitivity is not inversely proportional to the natural frequency approximated by equation (5) of the accelerometers but depends on the open loop gain and the form of compensation.

$$\omega_n = \sqrt{\frac{K}{m}} \quad (5)$$

Hence one of the biggest advantages is that the nonlinearity introduced by the spring and damping components is reduced considerably if the proof mass stays at the central position. The sampled voltage determines the comparator output which indicates that the seismic mass has moved towards the top plate, the comparator switches levels such that feedback voltage is applied to the bottom plate and the seismic mass is pulled back towards its rest position. The digital bit stream output of the comparator is sent to the low pass filter where the input (acceleration) gets

generated from the digital bit stream as illustrated in the figure 2.



Micro-machined sensing [10] elements have such small dimensions that allow the electrostatic forces to be used as the restoring force. But since the electrostatic forces are inherently positive and attractive (the electrostatic forces are proportional to the square of the voltage), a negative feedback is difficult to generate. However this could be overcome by superimposing two electrostatic forces on the seismic mass such that the resultant force provides a negative feedback. Negative feedback relationship is non-linear due to the dependency of the electrostatic forces on the square of the voltage and inversely related to the square of the gap between the electrodes. Also care has to be taken that the feedback signals do not interact with the excitation signal required for the pick off arrangement.

Drawbacks of the closed loop accelerometers with digital feedback include limited stability for large deflections since the voltage is applied continuously to the electrode and non-linear feedback voltages, since the force depends on the square of the feedback voltage, and hence direct application of a proportional feedback voltage leads to the non-linear feedback. Two methods of reset action possible are separation of the signals in the time domain or in the frequency domain.

4.1 Effects of excitation voltage

The excitation voltage introduces non linearity in the system by changing the spring constant. The effective spring constant is due to the sum of mechanical and electrostatic feedback forces. The electrostatic feedback charges non-linearity with displacement from the rest position and hence introduces the non-linearity [6].

Therefore sensing voltage cannot be increased beyond a certain limit which results on the sensitivity that one can be achieved. The closed loop accelerometers sensing elements produces an output proportional to the capacitive imbalance in the bridge. The charge amplifier output thus is proportional to the acceleration. The sampler samples this output and decides the direction of feedback done by the comparator. If the seismic mass has moved more towards the top (bottom) plate

then a positive voltage is applied on the bottom (top) plate to pull it back towards the rest position.

5. SIGMA-DELTA ADC

The AD7732 core consists of a charge balancing sigma-delta modulator and a digital filter. The architecture is optimized for fast, fully settled conversion. This allows for fast channel-to-channel switching while maintaining inherently excellent linearity, high resolution, and low noise. The AD7732 is a high precision, high throughput analog front end. True 16-bit p-p resolution is achievable with a total conversion time of 500 μ s (2 kHz channel switching), making it ideally suitable for high resolution multiplexing applications. The part can be configured via a simple digital interface, which allows users to balance the noise performance against data throughput up to 15.4 kHz.

The analog front end features two fully differential input channels with unipolar or true bipolar input ranges to ± 10 V while operating from a single +5 V analog supply.

The part has an over range and under range detection capability and accepts an analog input overvoltage to ± 16.5 V without degrading the performance of the adjacent channels.

The differential reference input features "No-Reference" detect capability. The ADC also supports per channel system calibration options. The digital serial interface can be configured for 3-wire operation and is compatible with microcontrollers and digital signal processors. All interface inputs are Schmitt triggered. The part is specified for operation over the extended industrial temperature range of -40° C to $+105^{\circ}$ C. Other parts in the AD7732 family are the AD7734 and the AD7738. The AD7734 is similar to AD7732, but its analog front end features four single-ended input channels. The AD7738 analog front end is configurable for four fully differential or eight single-ended input channels, features 0.625 V to 2.5 V bipolar/unipolar input ranges, and accepts a common-mode input voltage from 200 mV to $AVDD - 300$ mV. The AD7738 multiplexer output is pinned out externally,

allowing the user to implement programmable gain or signal conditioning before being applied to the ADC.

5.1 Output noise and resolutionspecification

The AD7732 can be operated with chopping enabled or disabled, allowing the ADC to be programmed to either optimize the throughput rate or channel switching time or to optimize the offset drift performance. Noise tables for these two primary modes of operation are outlined below for a selection of output rates and settling times. The AD7732 noise performance depends on the selected chopping mode, the filter word (FW) value, and the selected analog input range. The AD7732 noise will not vary significantly with MCLK frequency.

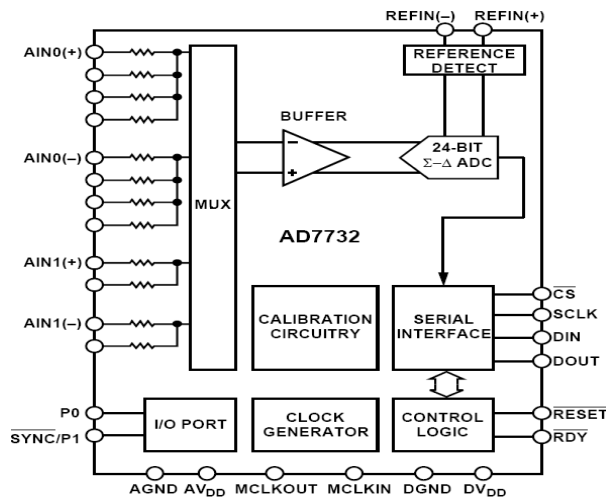


Fig 3: Block diagram of AD7732 sigma-delta chip

- **Chopping Enabled** - The first mode, in which the AD7732 is configured with chopping enabled (CHOP = 1), provides very low noise with lower output rates.
- **Chopping Disabled** - The second mode, in which the AD7732 is configured with chopping disabled (CHOP = 0), provides faster conversion time while still maintaining high resolution.

The peak-to-peak resolutions are not calculated based on rms noise but on peak-to-peak noise. These typical numbers are generated from 4096 data samples acquired in continuous conversion mode with an analog input voltage set to 0 V and MCLK = 6.144 MHz. The conversion time is selected via the channel conversion time register.

5.2 Frequency response

The sigma-delta modulator runs at 1/2 the MCLK frequency, which is effectively the sampling frequency. Therefore, the Nyquist frequency is 1/4 the MCLK frequency. The digital filter, in association with the modulator, features the frequency response of a first order low-pass filter. The -3 dB point is close to the frequency of 1/channel conversion time. The roll-off is -20dB/dec up to the Nyquist frequency. If chopping is enabled, the input signal is re-sampled by chopping. Therefore, the overall frequency response features notches close to the frequency of 1/channel conversion time. The top envelope is again the ADC response of -20dB/dec. The typical frequency response plots are given in Figure 4 and Figure 5. The plots are normalized to 1/channel conversion time.

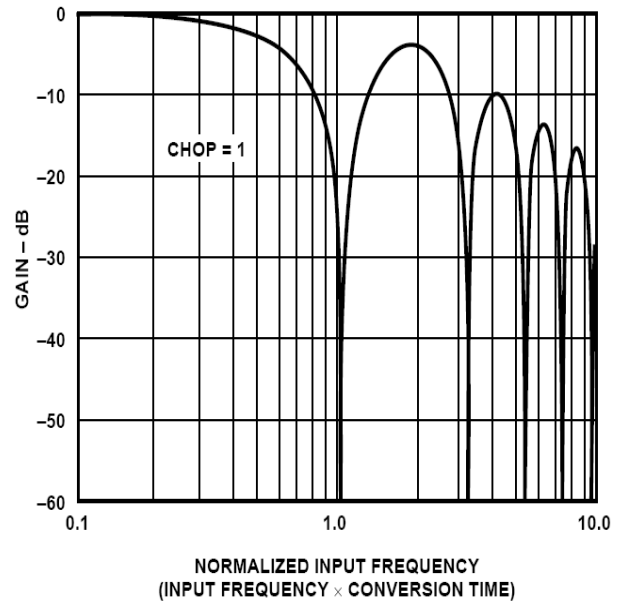


Fig 4: ADC Frequency Response, Chopping Enabled

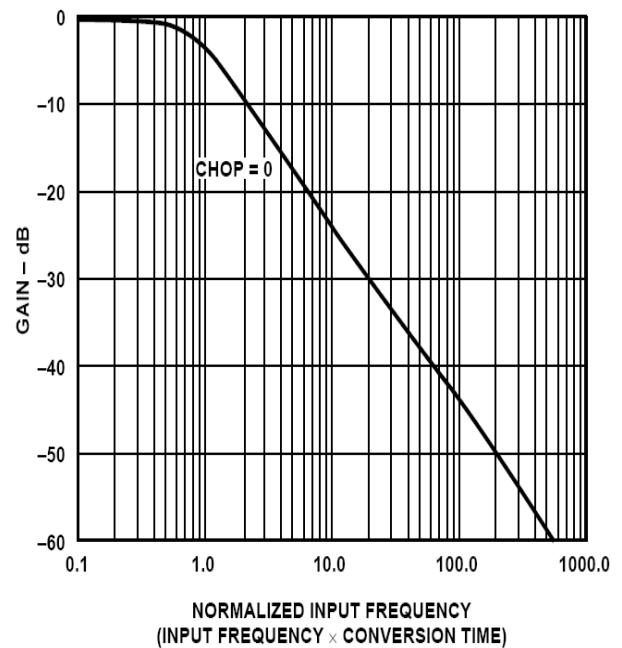


Fig 5: ADC Frequency Response, Chopping Disabled

5.3 ADC Zero-Scale Self-Calibration

The ADC zero-scale self-calibration can reduce the offset error in the chopping disabled mode. If repeated after a temperature change, it can also reduce the offset drift error in the chopping disabled mode.

The zero-scale self-calibration is performed on internally shorted ADC inputs. The negative analog input terminal on the selected channel is used to set the ADC zero-scale calibration common mode. Therefore, either the negative terminal of the selected differential pair or the single-ended channel configuration should be driven to a proper common-mode voltage. It is strongly recommended that the ADC zero-scale calibration register should only be updated as part of a zero-scale self-calibration.

6. RESULTS

Table 1 lists the test results. The drawbacks of the closedloop accelerometers with digital feedback can overcome by the sigma delta scheme where the feedback is constant voltage and the pulse width (the time of application) of the feedback is changed in the form of Pulse Width Modulation. Advantages of the closed loop accelerometers are the improved stability since voltage pulse is applied to only one electrode, the other electrode being grounded and even in a shock condition, the mass is eventually restored.

System Specifications

- Sigma delta converter chips (AD7732) is connected to the output of switched capacitor.
- O/P Voltage : 4.5V /2g
- Range : 2g
- Noise : 1mV
- Resolution : 453 μ g/0.416pF

Table 1. Tested Results

		C1 (pF)	C2 (pF)	C1~ C2 (pF)	Observed Vout (V)	Vout PSPICE
Ceramic capacitor		8.353	11.063	2.710	-0.339	-1.180
		11.063	8.353	2.710	1.869	1.010
Sensor (S1)	+1g	10.036	12.07	2.034	-0.127	-0.815
	-1g	10.979	10.79	0.189	0.705	-0.030
Sensor (S2)	+1g	9.957	11.371	1.414	0.050	-0.638
	-1g	11.542	9.849	1.693	1.280	0.532

From the results shown in figure 6, the lower linearity in the x-direction can be explained by the structure of the sensor. The even order nonlinearity is cancelled in the cases of y- and z-directions. The nonlinearity increased at higher accelerations due to the measurement setup. The measured response is shown in Fig. 7. The resultant of the accelerations to x- and y-directions corresponds to the earth's gravity, because the sensor is slightly slanted on the PCB. The angular acceleration and deceleration cause a tangential acceleration component that can clearly be seen in the y-directional acceleration curve.

The varying acceleration in y-direction is caused by the cogging torque.

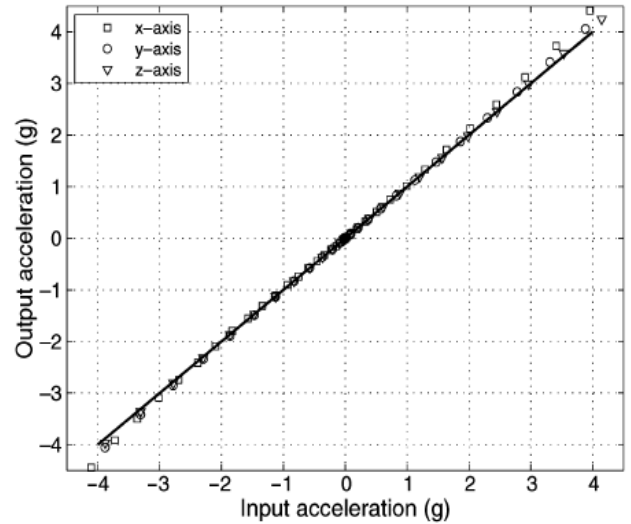


Fig 6: Measured dc acceleration in x-, y-, and z-directions.

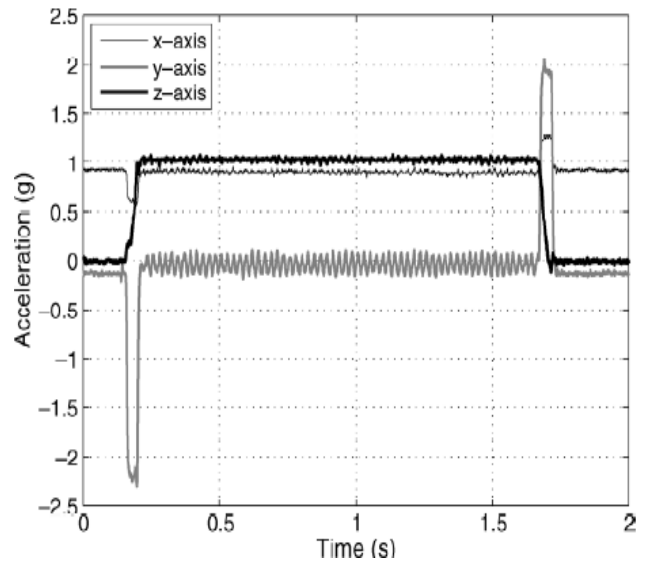


Fig 7: Acceleration pulse in z-direction

7. CONCLUSION

The open loop accelerometer has the limitations in terms of bandwidth, linearity and dynamic range. Moreover, non linear effects caused by the damping and the electrostatic forces required for the signal pick-off increase with the deflection of the seismic mass. One method of reducing these non linearities and improving the performance is to use the sensing element in a closed loop system in which a reset force is applied to the seismic mass to keep it at the central position between the electrodes.

Consequently, the force has to counterbalance the accelerating force and provide an accurate measure for the acceleration. In Micromachined sensing elements, the dimensions are such that electrostatic forces can be used to generate the restoring force. However since electrostatic forces are attractive, it is difficult to maintain negative feedback. Further complication is that the feedback relationship is inherently nonlinear because of the dependency of the electrostatic forces on the square of the voltage and the inverse square of the gap between the electrodes.

8. REFERENCES

- [1] Mikail Yüceta, Lasse Aaltonen, Mika Pulkkinen, Jarno Salomaa, Antti Kalanti, Kari Halonen. 2011. A Charge Balancing Accelerometer Interface with Electrostatic Damping in: ESSCIRC (ESSCIRC), 2011 Proceedings, Helsinki, 291–294
- [2] H. Luethold and F. Rudolf. 2000. An ASIC for High-resolution Capacitive Micro-accelerometers. *Sensors and Actuators*, vol. 21, 278-281.
- [3] M. Yüceta, L. Aaltonen and K. Halonen. 2010. Linearity Study of a Self-balancing Capacitive Half-bridge Sensor Interface. *Biennial Baltic Electronics Conference*, Tallinn, Estonia, 115-118.
- [4] J. Salomaa, et al. 2010. A $\Delta\Sigma$ ADC for Low Power Sensor Applications. In *Proceedings of IEEE International Symposium on Circuits and Systems*, Paris, 3100-3103.
- [5] Chau, K., Lewis, S.R., Zhao, Y., Howe, R.T., Bart, S.F. and Marcheselli, R.G. 1996. An integrated force balanced capacitive accelerometer for low-g applications. *Sensors and Actuators*, 472-476.
- [6] Burstein, A. and Kaiser, W. J. 1996. Mixed analog-digital highly sensitive sensor interface circuit for low-cost microsensors. *Sensors and Actuators*. 193-197,
- [7] Lewis, C. P., Kraft, M. and Hesketh, T. G. 1996. Mathematical Model for a Micromachined Accelerometer. *Transaction Institute of Measurement and Control*. Volume- 18, Issue 2. 92-98.
- [8] van Kampen, R. P. Vellekoop, M., Sarro, P. and Wolffenbuttel, R. F. 1994. Application of electrostatic feedback to critical damping of an integrated silicon accelerometer. *Sensors and Actuators*. 100-106.
- [9] B. V. Amini, R. Abdolvand, and F. Ayazi. 2006. closed-loop micro-gravity CMOS SOI accelerometer. *IEEE J. Solid-State Circuits*, volume 41, Issue no. 12, 2983–2991.
- [10] B. V. Amini and F. Ayazi. 2004. A 2.5-V 14-bit CMOS SOI capacitive accelerometer. *IEEE J. Solid-State Circuits*, volume 39, Issue no. 12, 2467–2476.